

Article

Not peer-reviewed version

---

# Detection Ground Deformation characteristics of Reclamation Land with Time-Series InSAR in Tianjin Binhai New Area, china

---

[Yanan Chen](#) , [Fu Li Yan](#) \* , [Jian Chen](#) , [Tao Xiang Fan](#)

Posted Date: 7 September 2023

doi: 10.20944/preprints202309.0535.v1

Keywords: Ground Settlement; Marine Reclamation Land; SBAS-InSAR; Tianjin Binhai New Area



Preprints.org is a free multidiscipline platform providing preprint service that is dedicated to making early versions of research outputs permanently available and citable. Preprints posted at Preprints.org appear in Web of Science, Crossref, Google Scholar, Scilit, Europe PMC.

Copyright: This is an open access article distributed under the Creative Commons Attribution License which permits unrestricted use, distribution, and reproduction in any medium, provided the original work is properly cited.

Article

# Detection Ground Deformation Characteristics of Reclamation Land with Time-Series InSAR in Tianjin Binhai New Area, China

Yanan Chen <sup>1,2</sup>, Fuli Yan <sup>2,\*</sup>, Jian Chen <sup>1</sup> and Xiangtao Fan <sup>2</sup>

<sup>1</sup> College of Engineering and Technology, China University of Geosciences-Beijing, 029 Xueyuan Road, Beijing 100083, China

<sup>2</sup> Aerospace Information Research Institute, University of Chinese Academy of Sciences, 009 Deng Zhuang South Road, Beijing 100094, China

\* Correspondence: yanfl@radi.ac.cn; Tel.: +86-13691957215

**Abstract:** In order to alleviate the conflict between populations and land-resource, Tianjin has adopted multi-phase reclamation projects to formed large-scale artificial reclamation land. However, the reclamation areas are susceptible to subsidence, which demonstrate a serious threat to infrastructure and people's lives and property. The SBAS-InSAR was used to acquired surface deformation of Tianjin Binhai New Area from January 2017 year to December 2022 year, analyzed in depth the response relationship between land subsidence and reclamation projects time as well as the land use type. The results show that the Lingang Industrial Zone was the earliest to be reclaimed, with extensive reclamation completed by 2016 year, while Nangang Industrial Zone and Hangu Port started reclamation projects in 2009 year, some areas are still currently under construction. There is a strong correlation between surface deformation and reclamation time, the severe land subsidence occurred over newly reclaimed areas. Surface deformation gradually intensifies from west to east, the maximum surface settlement in Nangang Industrial Zone, Lingang Industrial Zone from the west to the east has changed from -50 mm to -890 mm, 45 mm to -580 mm, respectively, reclamation area of Hangu Port with maximum surface deformation is -250 mm. Significant differences deformation among different land use types, which reclamation projects completed in the same time. Subsidence is positively correlated with surface load, in areas with higher surface loads, the surface settlement is also severer, the average surface settlement for the heavy shipyard, 67 grain storage tanks, 27 grain storage tanks, road, and bare land are -201 mm, -166 mm, -107 mm, -64 mm, and -43 mm, respectively. This study reveals significant differences of surface deformation in the reclamation completed at different times and the load is the main driving factor of settlement difference in the reclamation land completed at the same time. Which has important guiding significance for preventing and controlling geological disasters in the reclamation area and later development planning.

**Keywords:** ground settlement; marine reclamation land; SBAS-InSAR; Tianjin Binhai New Area

## 1. Introduction

With the rapid development of urbanisation, Tianjin's demand for land resources has risen sharply, Tianjin Binhai New Area has expanded its urban space through multiple phases reclamation projects [1]. Both dredger fill layer and underlying soil layer will undergo consolidation compaction, and the compaction of the sedimentary strata is considered to be an important factor causing land subsidence in the reclamation land [2]. However, there is a strong correlation between the degree of soil consolidation and completion time of the land reclamation project [3]. Significant differences in surface deformation have been observed in reclaimed areas completed at different time points. For example, surface deformation in the early reclaimed areas of Xiamen Airport shows relative stability [4]. The artificial reclamation area of Shanghai's Chongming Island expanded from west to east and surface subsidence rate also showed a trend of gradually increasing from west to east [5]. Shanghai Lingang New City

completed in 1973 year exhibit excellent surface stability, while significant deformation has occurred in completed reclamation projects after 2002 year [6].

At the same time, Tianjin reclamation is important industrial zone and the maritime gateway of the national shipping centre in North China, a large number of factories, ports, and buildings have been constructed on the surface. The continuous load of surface structures provides a good foundation for the development of land settlement. Additional load from buildings is one of the factors causing land subsidence in urban areas[7,8]. The buildings in Wuhan industrial zone are dense and the surface load is large, which results in significant ground settlement[9]. Artificial reclamation area at Shanghai Pudong Airport, surface deformation is greater in areas where large quantities of goods are stockpiled[10]. Under combined effects of soil consolidation and surface building load, land subsidence in Tianjin Binhai New Area is inevitable. However land subsidence is difficult to recover, and it can lead to secondary hazards such as coastal erosion[11], seawater intrusion[12], and soil salinization[13,14]. It also increases the risk of instability for artificial structures, weakens the stability of infrastructure such as roads, railways, buildings, dams [15], and submarine tunnels, and shortening their service time. Therefore, determine the magnitude of surface deformation in different time completed reclamation land and analyze surface deformation characteristics of different land use types have great significance for prevention and control of land subsidence hazard, ensuring the safety of buildings, planning and design of surface construction in the next phase of Tianjin Binhai New Area land reclamation.

Currently, domestic and foreign scholars' studies on Tianjin mainly focus on surface deformation characteristics in the main urban area[16], the long time series of groundwater level changes[17,18], and the response relationship between surface deformation and groundwater level changes[19,20], there are important for the development of land resources and ensuring the safety of infrastructure in Tianjin. However, groundwater exploitation has not been carried out in the reclaimed areas of Tianjin Binhai New Area. The existing settlement analysis of the urban area cannot explain the settlement characteristics of the Binhai New Area, meanwhile not analyze in-depth the differences in ground deformation between reclamation completion time and different land use types. In order to provide a basis for the settlement management and engineering control measures, it is particularly urgent to further investigate the settlement driver factor in Binhai New Area.

Large-scale artificial reclamation in Tianjin Binhai New Area, traditional surface deformation measurement methods such as Leveling, GNSS, Borehole Extensometers, and Tilt measurement can obtain high-precision surface deformation, but they are all point-based measurements and difficult to acquire high-precision spatially continuous large-scale deformation. In addition, the cost is expensive [21]. In recent years, with the development of synthetic aperture radar interferometry technology, SBAS-InSAR (small baseline subset interferometric synthetic aperture radar) has been widely used in ground deformation detection with high-precision, large-scale, low cost[9,23–26].

In summary, the artificial reclamation land in Tianjin Binhai New Area has a significant risk of ground subsidence. Currently, there has been no exploration of surface deformation patterns in the reclamation area, which fails to meet the requirement of disaster prevention and later land resources development in the reclamation area. The high-precision SBAS-InSAR is employ to detect the spatio-temporal deformation, Landsat-5, Landsat-7 and Landsat-8 from 1986 year to 2022 year are use to acquire coastline changes and GF-1 and GF-2 from 2018 year to 2022 year are use to identify land use types of reclamation in Tianjin Binhai New Area. Combined with the reclamation projects time and land use types, the driving factors of surface deformation be analyzed. It has important practical significance for ensuring the safety of infrastructure, preventing geological disasters, and planning the design of artificial reclamation in Binhai New Area.

## 2. Study area

Tianjin Binhai New Area is located in the northwestern part of Bohai Bay, the geomorphology consists of intertidal plain and marine low plain, coastline is low and straight, and gradually decreases

from west to east [27]. The main geological formation is made up of unconsolidated Quaternary and Upper Neogene deposits [28]. The Quaternary sediments primarily consist of alluvial and marine deposits[29]. There is widespread distribution of coastal sediments on the surface, mainly composed of silty clay and loamy clay, with large pore, high moisture content, mostly showing soft plasticity and low strength[30].

According to the "Urban Master Plan of Binhai New Area," the total area of reclamation in Binhai New Area reached 413.6 km<sup>2</sup> in 2020 year. A large number of ports, factories, petrochemical plants, residential buildings, grain and oil refining plants have been built in the reclaimed area, which implement the transshipment and transportation of bulk goods such as containers, crude oil, minerals, and coal. It serves as the marine gateway for the North China Plain[31] and holds a significant strategic position. Reclamation land of Binhai New Area can be divided into Nangang Industries Zone, Lingang Industries Zone, and Hangu Port in Figure 1. Nangang Industries Zone is the largest reclamation port [32] and The Lingang industrial zone is the maximal comprehensive trade port in northern China.

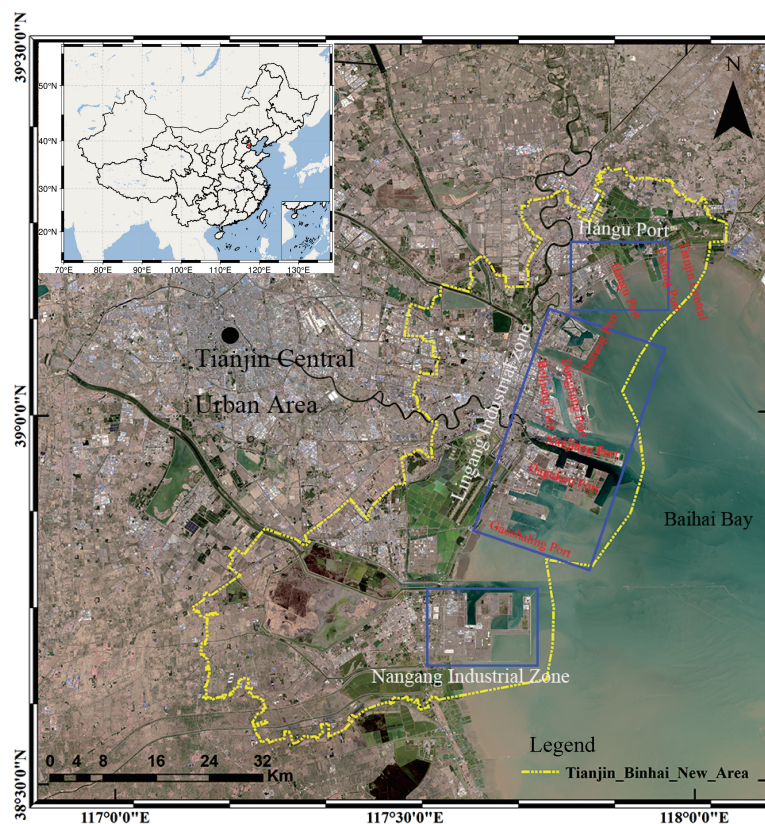


**Figure 1.** Location map of Tianjin Binhai New Area. The blue rectangle represent Nangang Industrial Zone, Lingang Industrial Zone and Hangu Port.

### 3. Data and Methodology

#### 3.1. Datasets

A total of 159 Sentinel-1A images from January 3, 2017 year to December 27, 2022 year were obtained to monitor ground deformation characteristics and spatial distribution in the reclamation area of Tianjin Binhai New Area. Landsat5, Landsat7, Landsat8 images from 1986 year to 2023 year was applied to identify the coastline changes, GF-1, GF-2 from 2018 year to 2022 year were used to identify the land use types. The information of the acquired image dataset is shown in Table 1.

**Table 1.** Basic parameters of images data set

Image	Temporal coverage(year)	Number of images	Resolution(m)	Purpose
Sentinel-1A	2017-2022	159	20	Ground Deformation Detection
Landsat-5	1986-2011	35	30	Coastline Change Identification
Landsat-7	2012	5	30	Coastline Change Identification
Landsat-8	2013-2022	29	30	Coastline Change Identification
GF-1	2019-2022	23	2	Land Use Types Identification
GF-2	2018-2019	4	0.8	Land Use Types Identification

### 3.2. Methodology

SBAS-InSAR was used to acquired ground deformation. The principle of SBAS-InSAR is divide all SAR images obtained in the same area into several small subsets that satisfy the requirements of both temporal and spatial baselines[33–35]. The least square method is used to solve the phase in each set, and then the remaining small baseline sets are combined, Singular Value Decomposition(SVD) is used to slove multiple small baseline sets to obtain the least square solution under the smallest norm, then obtain the time series deformation sequence in the study area[36–38]. To avoid temporal and spatial decorrelation, time baseline threshold of 60 days and a spatial baseline threshold of 10% were set. A total of 710 image pairs were acquired from January 2017 year to December 2022 year, as shown in Figure 2. Multi-viewing and Goldstein filtering were applied for noise removal. The Shuttle Radar Topography Mission digital elevation model with a resolution of 30 m was used to remove topography phase. Precise Orbit Data (POD) provided by the European Space Agency (ESA)<https://qc.sentinel1.eo.esa.int>, were used to remove orbit error. The Delaunay MCF method was used for phase unwrapping.

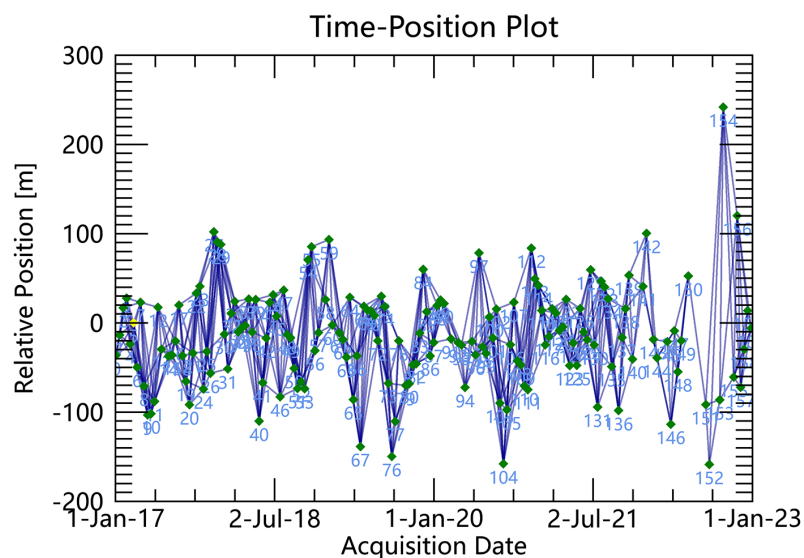


**Figure 2.** Interferogram pairs formed by Sentinel-1A data sets. The green Squares and blue lines represent the image and interferometric pairs, respectively. The yellow dot refers to the super master image.

A coherence-based method was used to estimate precision measurement.

$$\text{precision} = \sqrt{\frac{1 - \gamma^2}{2\gamma^2}} \times \frac{\lambda}{4\pi} \quad (1)$$

Where  $\gamma$  is the interferometric coherence, and  $\lambda$  is the wavelength of the C-band Sentinel1-A(5.6 cm).

Geometric and atmospheric corrections were applied to the optical images in table 1. Landsat-5, Landsat-7, Landsat-8 from 1986 year to 2023 year were used for identify coastline change by visual interpretation, and surface construction type was identified by combining the GF-1 and GF-2 images and high-precision electronic map.

#### 4. Results and Discussion

##### 4.1. SBAS-InSAR Results and Validation

The coherence-based method mentioned in Section 3.2 was used to validate the SBAS-InSAR accuracy. Figure 3 display the precision value of land surface deformation in Tianjin Binhai New Area is between 0.1 and 1.9, furthermore, the artificial reclamation area is in the range of 0.1 to 1.4. Precision values within the range of 0 to 3 are considered reliable[39–41], therefore, the surface deformation obtained by SBAS-InSAR in this study is reliable.

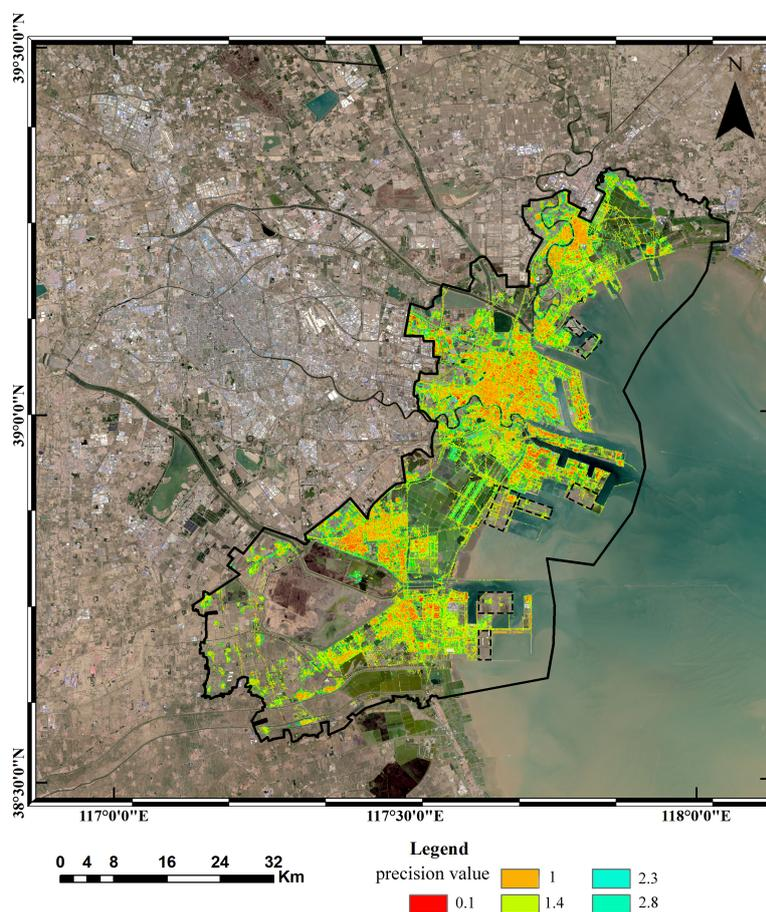


Figure 3. The SBAS-InSAR precision value of Tianjin Binhai New Area

Ground deformation in Tianjin Binhai New Area from January 3, 2017 year, to December 27, 2022 year was extracted, as shown in Figure 4. Significant spatial variation in surface deformation, there is gradual intensification of surface subsidence from west to east in all port areas. The maximum settlement in the western of Nangang Industrial Zone is -50 mm, in the east is -890 mm. The maximum deformation in the western of Lingang Industrial Zone is 45 mm, in the east is -580 mm. Hangu Port upward from east to west, the maximum subsidence from -170 mm to -250 mm.

Additionally, less surface deformation information was obtained in Figure 4 marked by the black dashed rectangle, and these areas not detect the precision value in Figure 3. Figure 5 reveals these areas of red rectangular marked area in (f) experienced seawater intrusion after completed of the reclamation project. The reclaimed area's soil was eroded by seawater, resulting in surface water infiltration. Multi-phase reclamation project were taken in these areas, leading to less land deformation information observed in Figure 4.

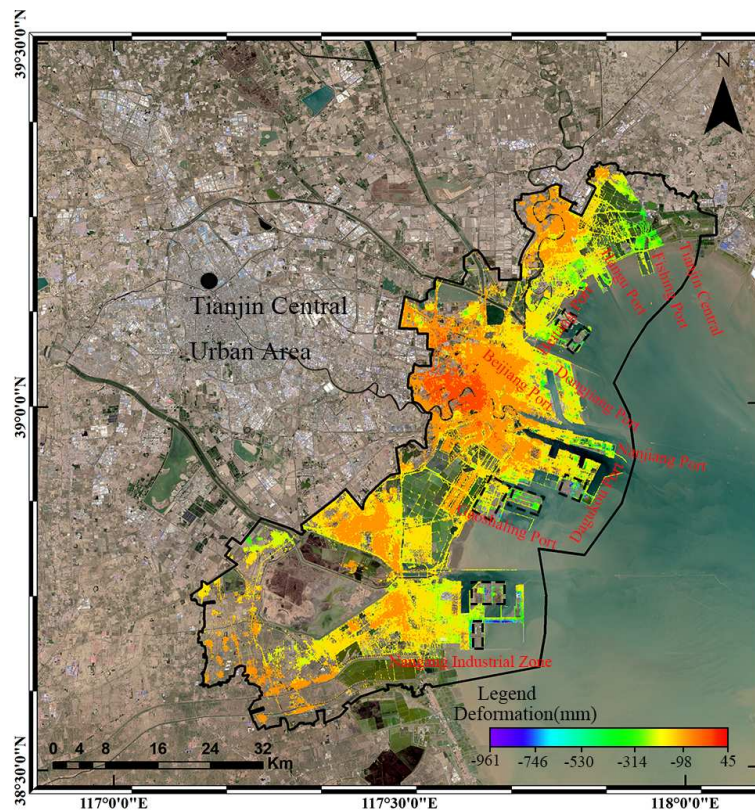
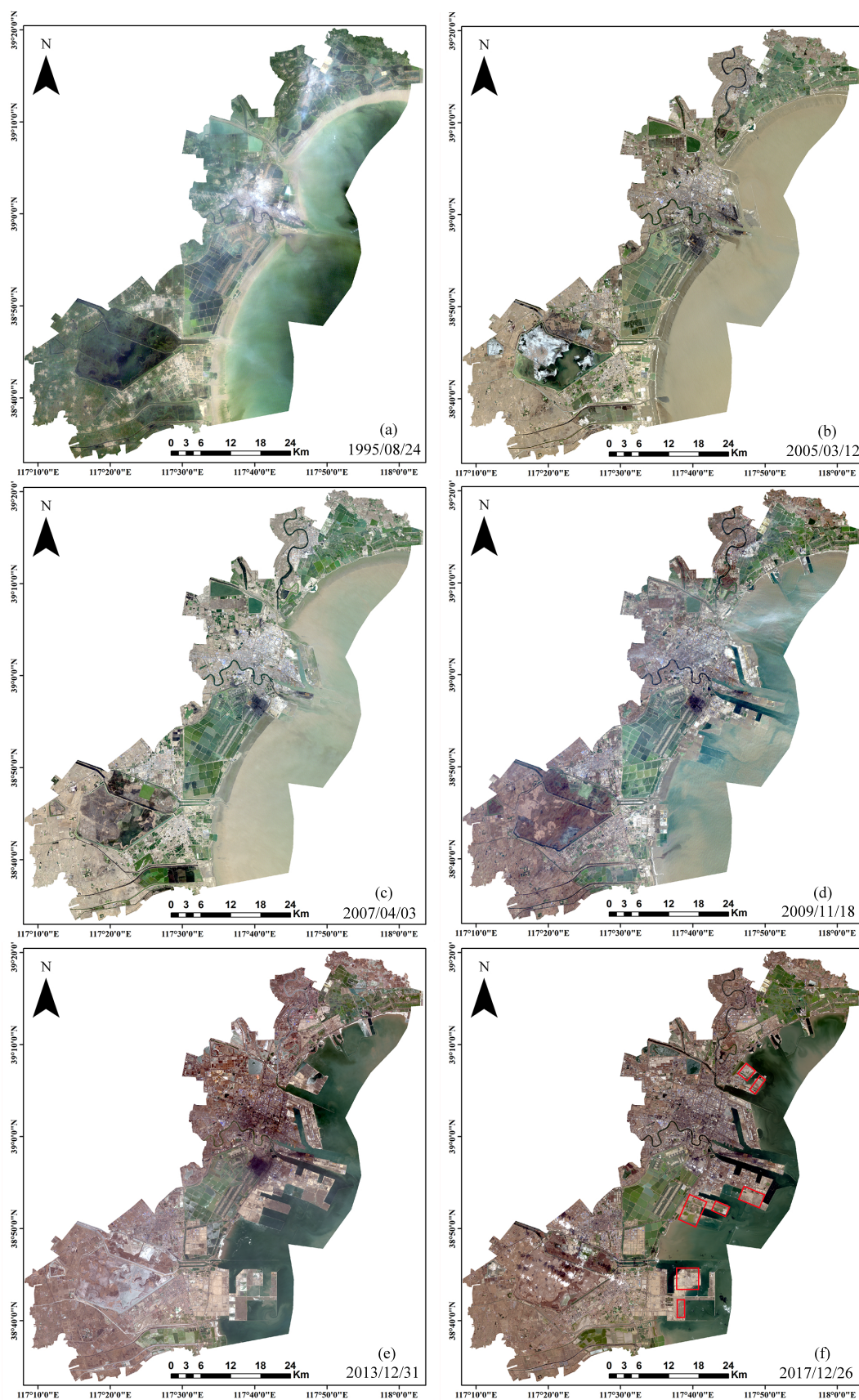


Figure 4. SBAS-InSAR deformation results.

#### 4.2. Land Reclamation Spatial Evolution at Tianjin Binhai New Area

Figure 5 shows the spatial evolution history of land reclamation in Tianjin Binhai New Area. In Figure 6. Reclamation in Lingang Industrial Zone started the earliest, with Beijiang Port completed in 1995 year, while all ports in Lingang Industrial Zone, except Gaoshaling Port, were completed in 2014 year. The reclamation project in Nangang Industrial Zone began in 2009 year and was mostly completed by 2022 year. Hangu Port's reclamation started in 2009 year and was completed in 2014 year, while Tianjin Central Fishing Port was still under construction in 2022 year.

The reclamation area for each time point was calculated. The results are shown in Figure 7, it can be observed that the artificial reclamation acreage was relatively large in 2009 year, 2010 year, and 2014 year, with 56.265 km<sup>2</sup>, 61.441 km<sup>2</sup>, and 56.548 km<sup>2</sup>, respectively. Artificial reclamation area gradually increased from 1995 year to 2010 year and reached peak in 2010 year. From 2015 year to 2022 year, artificial reclamation area significantly decreased, indicating a recent decline of land reclamation activities in Tianjin Binhai New Area.



**Figure 5.** Spatial Evolution of Tianjin Binhai New Area Land Reclamation. The background image is from Landsat-5 and Landsat-8 satellites.

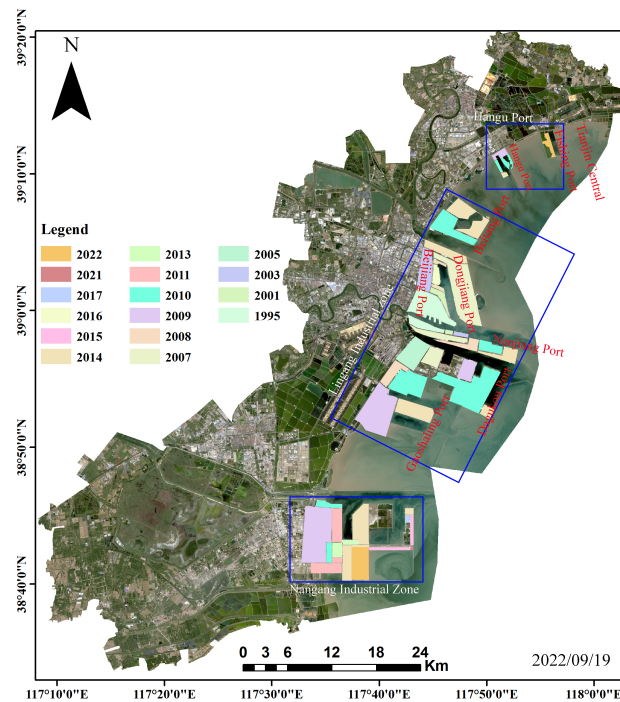


Figure 6. Statistical map of the spatial and temporal evolution of reclamation areas.

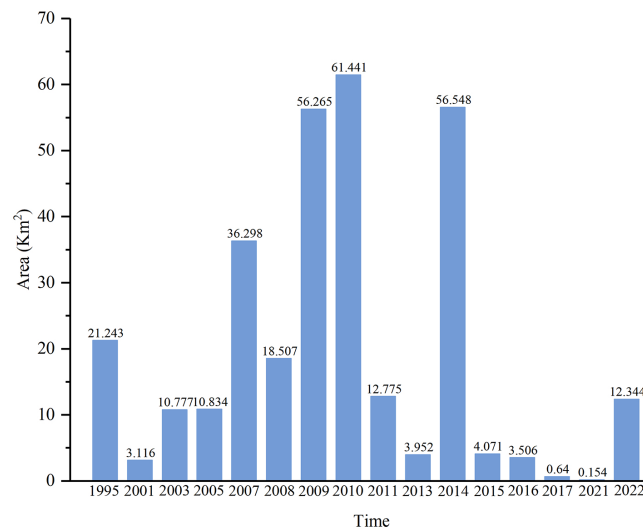


Figure 7. Reclamation area of Tianjin Binhai New Area.

#### 4.3. Responsive Relationship between reclamation time and surface deformation

Figure 8 provide amplified view of surface deformation of Nangang Industrial Zone, Lingang Industrial Zone and Hangu Port. the blue dashed rectangle in the Figure 8a experienced the most severe surface deformation, with a maximum surface deformation value of -890 mm, which reclamation Completed in 2015 year. There is a significant spatial difference of surface deformation in Nangang Industrial Zone, with a trend of severe subsidence from west to east. In the reclamation completed in 2009 year, the surface deformation was around -98 mm, significantly smaller than the area completed at later stage.

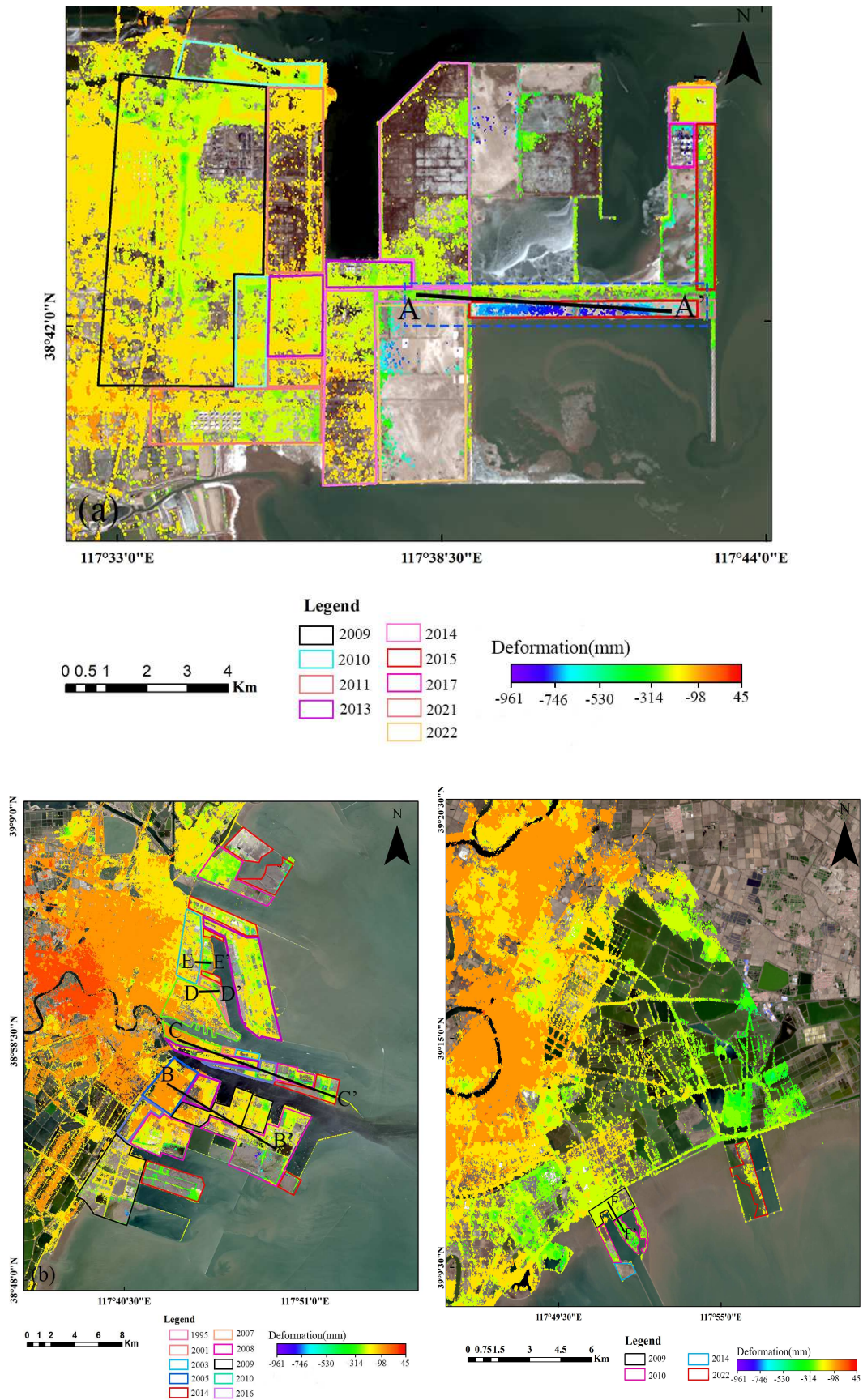


Figure 8. Ground deformation rate map.(a)Nangang industrial zone.(b)Lingang industrial zone.(c) Hangu Port

From Figure 8b, the artificial reclamation in Lingang Industrial Zone gradually expanded from the western to eastern, and there are also significant differences of surface deformation in the east-west direction. The surface deformation in the western reclamation area range from 45 mm to -98 mm, while in the eastern region, it range from -526 mm to -456 mm. The areas completed in 2010 year and 2014 year exhibited much greater subsidence compared to other time.

In Figure 8c, ground deformation of Hangu Port reclamation land completed in 2009 year, 2010 year are -140 mm to -160mm, and -178 mm to -290 mm, respectively. Tianjin Central Fishing Port is still under construction.

Additionally, the reclamation projects in Nangang Industrial Zone and Hangu Port are later than Lingang Industrial Zone, as a result, the surface settlement in most areas of Nangang and Hangu port are larger than Lingang Industrial Zone.

By comparing magnitudes of surface deformation and reclamation time in each area, it is evident that there is a high correlation between surface deformation and reclamation time. To quantify the differences in surface deformation among the reclamation areas completed at different time points, the cumulative surface deformation from January 2017 year to December 2022 year was extracted for the six black solid lines indicated in Figure 8. The results are shown in Figure 9.

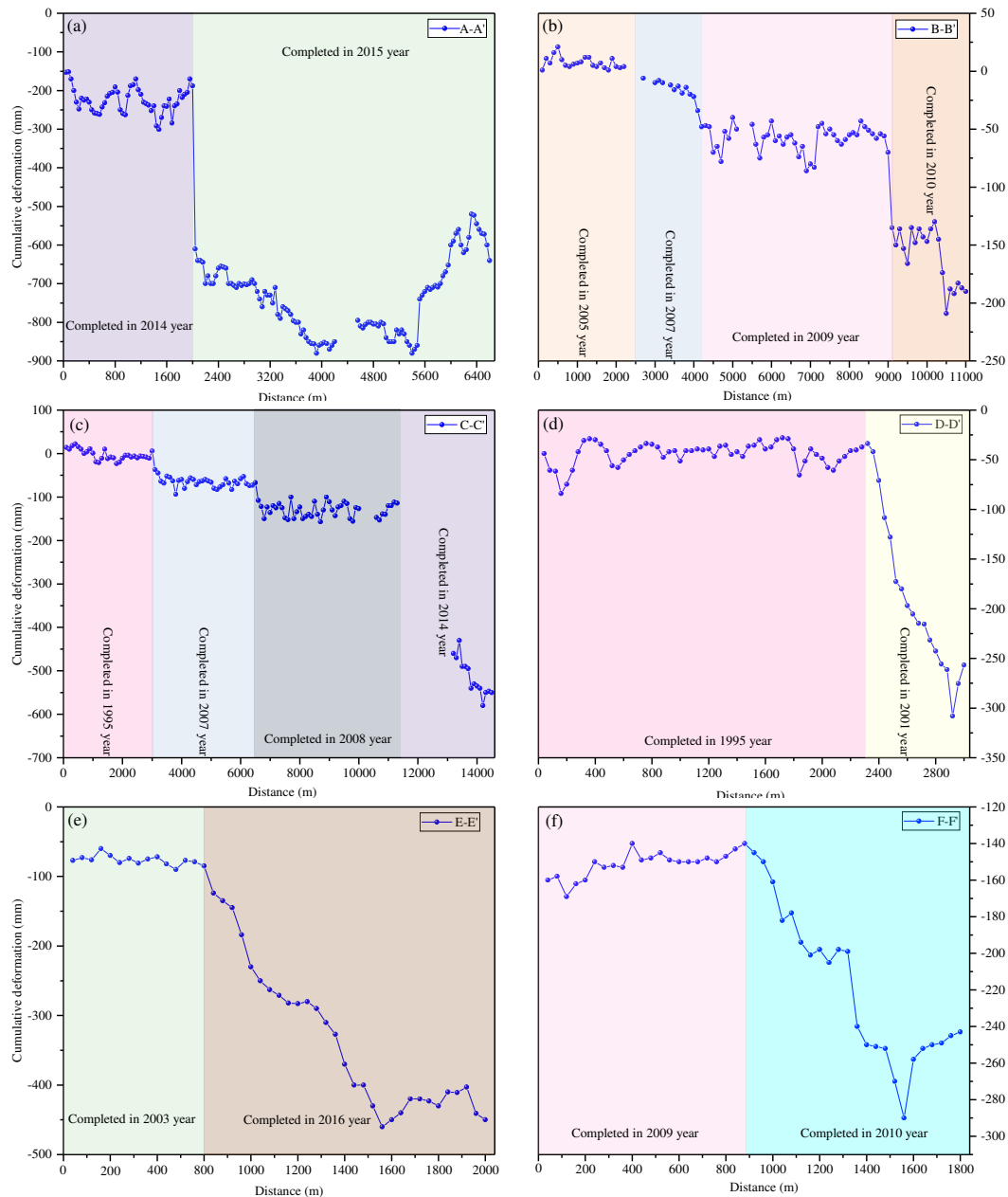


**Figure 9.** Cross-section of cumulative deformation of Tianjin Binhai New Area along six profiles from January 2017 year to December 2022 year, whose positions are marked in Figure 8. (a)Profile A-A'; (b)Profile B-B'; (c)Profile C-C'; (d)Profile D-D'; (e)Profile E-E';(f)Profile F-F'.

Figure 9 demonstrate the quantitative relationship between different land reclamation periods and surface deformation. Different background colors represent different completion times of land reclamation. Multiple surface subsidence funnels are observed in the areas where the six profile lines, with significant differences in subsidence magnitudes among different regions.

On Profile A-A', the surface deformation in the reclamation area completed in 2014 year range from -152 mm to -301 mm and the most severe surface deformation is completed in 2015 year, range from -610 mm to -890 mm. On Profile B-B', ground deformation in the reclamation area completed in 2005 year,2007 year, 2009 year and 2010 year are range from 1 mm to 22 mm, -8 mm to -48 mm, -50 mm to -86 mm and -130 mm to -209 mm, respectively. On Profile C-C', the surface deformation in the reclamation area completed in 1995 year range from 1 mm to -12 mm, while in 2007 year it ranges from -37 mm to -94 mm, in 2008 year it range from -105 mm to -152 mm, and in 2014 year it range from -460

mm to -550 mm. On Profile D-D', the surface settlement in the reclamation area completed in 1995 year range from -31 mm to -70 mm, and in 2001 year it range from -76 mm to -330 mm. On Profile E-E', the ground subsidence in reclamation land completed in 2003 year ranges from -60 mm to -90 mm, while in 2016 year it ranges from -124 mm to -460 mm. On Profile F-F', the ground settlement of artificial reclamation land completed in 2009 year and 2010 year are -140 mm to -160mm, and -178 mm to -290 mm, respectively.

To further reveal the surface deformation patterns of the reclaimed land, this study extracted time series deformation of four points (P1-P4) shown in Figure 11. The results are presented in Figures 10. Among them, P1, P2, P3, and P4 are located in bare land. From Figure 10, it can be seen that the surface cumulative deformation for the bare land reclaimed in 2007 year, 2010 year, 2014 year, and 2015 year are -40 mm, -201 mm, -281 mm, and -871 mm respectively, indicating a significant trend of severe surface deformation in the areas where reclamation was completed later. Although the bare land areas in Tianjin Binhai New Area have not been developed, the fill soil itself will cause consolidation, and the dredged soil as a large-scale load will cause compression deformation in the underlying layers. The weak soil layer will also experience secondary consolidation under the long-term loading of the fill soil[42], resulting in significant settlement in the bare land areas of the study area.

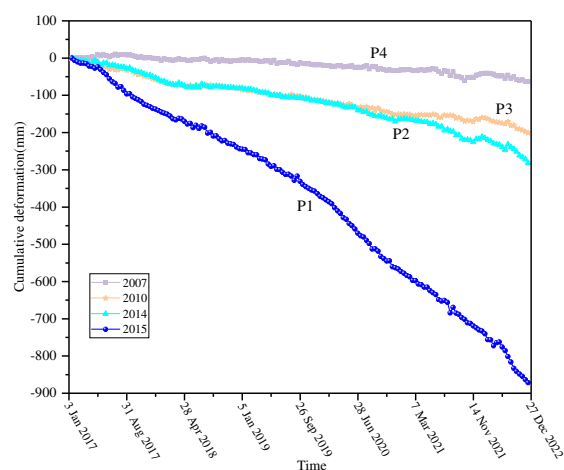


Figure 10. Bare land time series deformation.

All six profiles cumulative deformation and the time series deformation of the bare land further demonstrate a strong correlation between surface subsidence and the time of reclamation. The earlier reclamation project is completed, the consolidation of the fill and the compression of the underlying soil layer will tend to be stable, resulting in less surface subsidence. Conversely, the severe land subsidence occurred over newly reclaimed areas. A similar phenomenon was observed in the reclamation land of Xiamen new airport [4].

At the same time, in Figure 9a,c, the surface settlement for the areas reclaimed in 2014 year are -152 mm to -301 mm, and -460 mm to -550 mm respectively. In Figure 9c,d, the surface deformation for the areas reclaimed in 1995 year are 1 mm to 22 mm and -31 mm to -70 mm. In Figure 9b,c, the surface subsidence of reclamation completed in 2007 year are -8 mm to -48 mm and -37 mm to -94 mm respectively. Figure 9b,f reclamation completed in 2009 year, the ground deformation are -30 mm to -98 mm, -140 mm to -160 mm, respectively. This indicates significant variations in surface deformation among reclamation areas completed at same times in different regions.

#### 4.4. Relationship between Land Use Types and Deformation

In order to investigate the spatial differences in ground settlement for reclamation completed at the same time. GF-1 and GF-2 images were used to identify the land use types as shown in Figure 11. From Figure 11, it can be observed that the main land use types in the reclamation areas are petrochemical plants, industrial areas, residential areas, cargo storage areas, and mineral storage areas.

The unmarked reclamation areas are bare land. Higher degree of industrialisation in the Lingang Industrial Zone, with a larger number of factories and cargo storage areas. The land use type of the Nangang Industrial Zone are bare land, petrochemical plants, factories and mineral storage areas. The Hangu Port reclamation area has very few factories.

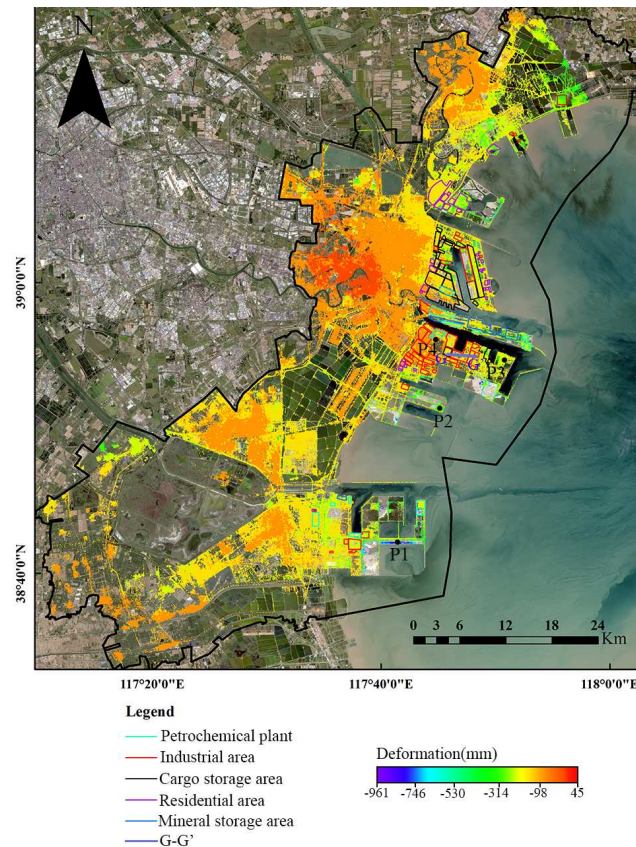


**Figure 11.** Surface construction types deformation, with different color solid boxes representing different surface construction types. The black points are the sampling points for extract time series deformation. points P1, P2, P3, and P4 are bare land, and the reclamation time is 2015 year, 2014 year, 2010 year, and 2007 year, respectively.

According to Figure 9, significant differences in surface deformation were observed in the reclamation areas completed in same time. In Figure 11, the land use types in the reclamation area completed in 1995 year along profile lines C-C' and D-D' in Figure 9 are factories and cargo storage areas. The cargo storage area on profile line E-E' includes Chihaikia Car Ro-Ro Terminal and Tianjin Maoxin Storage Yard. Due to long-term static load from bulk cargo storage and dynamic load from transportation of goods such as vehicles, the subsidence of the cargo storage area is greater than that of the factory area. On figure 9 profile line B-B', which the reclamation area completed in 2007 year, surface subsidence is smaller compared to C-C'. According to Figure 11, the surface construction types along profile lines B-B' and C-C' are bare land and mineral storage area, respectively. The mineral storage area has a large amount of mineral piles on the surface, which imposes a large surface load. Additionally, the bare land on profile line B-B' was reclaimed earlier, surface deformation relatively stable.

Combining the surface deformation characteristics of different construction types in Figures 9 and Figure 11, it can be concluded that the land use types is the main reason for the significant difference in the deformation of reclamation areas completed at the same time. To further analyze the differences in surface deformation in the reclamation areas completed during the same period, extracted the deformation profile at the location of G-G' in Figure 11, and shown in Figure 12.

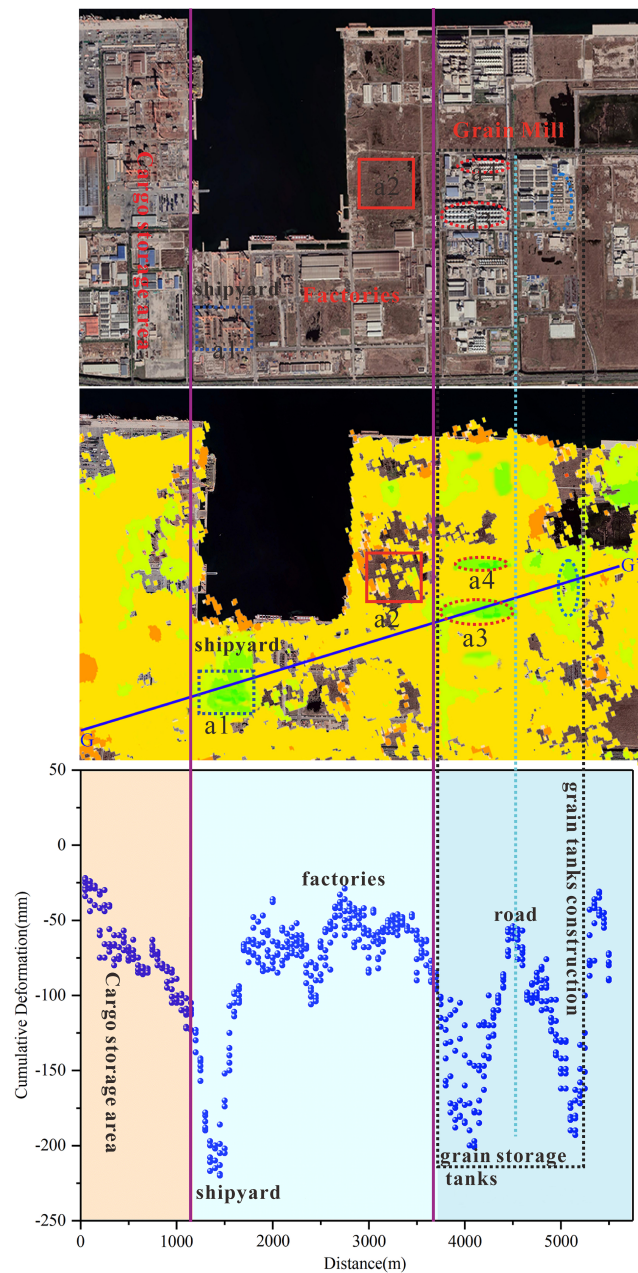


**Figure 12.** Cross-section of cumulative deformation of Lingang Industrial Zone along G-G' profiles from January 2017 to December 2022, whose positions are marked in Figure11.(a1)heavy shipyard, (a2)bare ground, (a3)67 grain storage tanks and (a4)27 storage tanks.

According to Figure 12, there is a subsidence funnel with a maximum subsidence of -220 mm in the blue dashed rectangle, which is Lingang shipyard and China Shipbuilding (Tianjin) Ship Manufacturing Co., Ltd. It can be seen from the optical image that a crane is located in the blue dashed rectangle area for large-scale ship movement and assembly, the surface load is large. In the factory zone, the surface deformation is relatively minor, it is due to the factory occupies a large area and sparse buildings distribution, resulting in a dispersed surface load. The black dashed rectangle represents Jingliang (Tianjin) Grain and Oil Industry Co., Ltd., which has two grain and oil plants. The two subsidence funnels align with the locations of the plants. In the surface deformation map, the red dashed elliptical area shows significant surface deformation, and from the optical image that two grain storage tanks are placed in these elliptical areas, creating a high and concentrated surface load. The cyan dashed elliptical area represents the ongoing construction of grain storage tanks, higher

anthropomorphic disturbances resulting in severe surface settlement. The cyan dashed line is located at the intersection of the subsidence funnels of the grain plants, showing relatively small surface deformation. Based on the optical image, this area corresponds to a road, with a smaller surface load compared to the area where the grain storage tanks are located. The surface subsidence in the cargo storage area ranges from -75 mm to -90 mm. It can be observed from the optical image that this area belongs to a logistics company, but the number of containers is small. Based on the above information, it can be concluded that significant subsidence will occur in areas with high surface load.

In Figure 12, a1 is located in the heavy shipyard, and a2 is bare land without any building, and there is no surface water seepage phenomenon observed in area a2 based on optical image. Both a3 and a4 are located at the grain storage tanks, the number is 67 and 27, respectively, and from Optical images specification and size of the storage tanks is same. To compare the surface deformation characteristics under different surface loads, this study randomly and uniformly selected 20 points from locations a1, a2, a3, a4, and road to extract the average surface settlement, result shown in Figure 13.

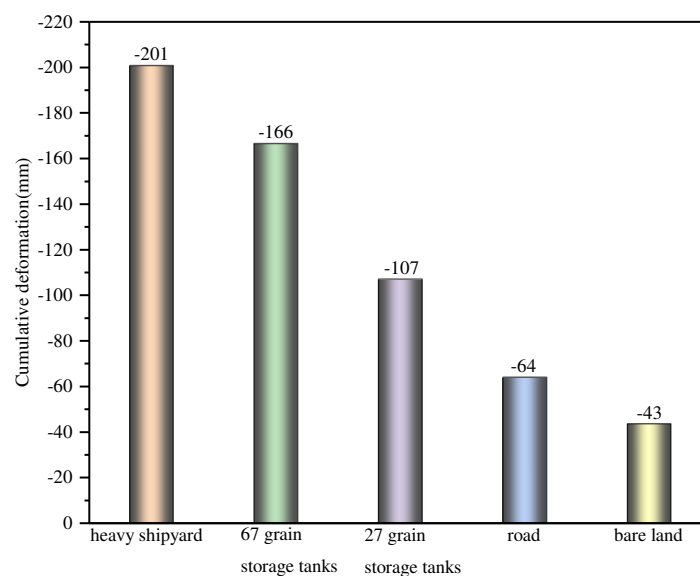


**Figure 13.** Average ground settlement for different land use types with reclamation completed at the same time.

From Figure 13, the average surface settlement gradually decreases in the five areas. The average settlement in the heavy shipyard area is the largest with -201 mm. A large amount of steel for shipbuilding has been piled up in the area, and a large number of cranes have been built on the surface for assembling ships, which can be regarded as a great surface load in this area. In the two grain and oil tank areas, the surface load in the area with 67 tanks is greater than that in the area with 27 tanks, with average settlements of -166 mm and -107 mm, respectively. The road is a necessary route for the grain and oil transportation of Beijing Grain (Tianjin) Industry Co., Ltd., and there are many vehicles. However, the surface load is much smaller than the grain storage tank areas and the heavy shipyard, with an average settlement of -64 mm. The bare land area is undeveloped with no surface loading and average surface settlement of -43 mm. Combining the surface load and surface settlement in these five areas, it can be observed that there is a positive correlation between surface load and surface settlement. The greater the surface load, the larger surface settlement.

In summary, different land use types lead to significant differences in surface deformation of the reclaimed area completed at the same time. the larger the surface load, the greater the surface settlement. In order to ensure the safety of buildings in the reclaimed area, intensive monitoring should be carried out for heavy industrial areas with large surface loads. When developing and utilizing reclaimed areas, heavy plants should be planned to avoid areas of serious surface settlement, and foundations should be compacted and reinforced before construction.

## 5. Conclusions

In order to satisfy the requirement of disaster prevention and control in the reclaimed area of Tianjin Binhai New Area and the rational development of land resources in the later stage, SBAS-InSAR method was employed to process 159 Sentinel-1A from 2017 year to 2022 year and surface deformation was detected. A coherence-based method was used to validate the accuracy of surface deformation, with a precision range of 0.1-1.9, indicating that surface deformation in this study is reliable. 69 scenes of Landsat-5, Landsat-7, and Landsat-8 images from 1986 year to 2022 year were used to interpret land reclamation process, The GF-1 and GF-2 from 2018 year to 2022 year were interpreted to obtain the main land use types, and main land use types are Petrochemical plant, Industrial area, Residential area, Cargo storage area, Mineral storage area and Bare land in the reclaimed area of Tianjin Binhai New Area. Combining the surface deformation obtained by SBAS-InSAR with the reclamation process, land use types, the article draws the following conclusions:

The reclamation land in Tianjin Binhai New Area shows the characteristics of expanding from west to east. Lingang Industrial Zone was the earliest started reclamation projects and completed most of reclamation areas in 2016 year, while Nangang Industrial Zone and Hangu Port started reclamation projects in 2009 year. The artificial reclamation area increased from 1995 year to 2010 year, reaching peak of 61.441 km<sup>2</sup> in 2010 year. The artificial reclamation area has significantly decreased from 2015 year to 2022 year, indicating a slow expansion of the reclamation area in recent years.

There is a significant correlation between surface deformation and reclamation time, the surface subsidence of newly completed reclamation areas is severe. The maximum surface settlement in Nangang Industrial Zone, Lingang Industrial Zone from the west to the east are from -50 mm to -890 mm, 45mm to -580mm, respectively. and the maximum surface deformation in the completed in 2009 year and 2010 year of Hangu Port is -160 mm, -290 mm, respectively. For new development in the reclamation land, careful consideration should be given to the scale and type of buildings.

There is a significant difference in surface subsidence among different land use types completed in the same time of reclamation areas. The average surface subsidence of heavy shipyards, 67 grain storage tanks area, 27 grain storage tanks area, road, and bare land are -201 mm, -166 mm, -107 mm, -64 mm, and -43 mm, respectively. This indicates that there is a positive correlation between surface load and surface subsidence, and the larger surface load, surface subsidence is more severer.

This article identifies the characteristics of surface deformation and reclamation history in Tianjin Binhai New Area, and analyzes in depth the relationship between reclamation time, surface construction types, surface load, and surface subsidence. The research results have important guiding significance for preventing geological hazards in the coastal area and later development and utilization of the reclamation area.

**Author Contributions:** C.Y. and Y.F. conceived the manuscript, C.Y. performed the experiments, interpreted the results and drafted the manuscript. C.Y., Y.F., and C.J. contributed to the discussion of the results. All authors conceived the study, and reviewed and approved the manuscript.

**Funding:** This research was supported by the National Key Research and Development Program of China (Grant No. 2022YFC330160207) and the Strategic Priority Research Program of the Chinese Academy of Sciences (Grant No. XDA19080101).

**Acknowledgments:** The Sentinel-1A data used in this study were freely provided by Copernicus and ESA, and the one-arc-second SRTM DEM data were freely downloaded from the website [http://e4ftl01.cr.usgs.gov/MODV6\\_Da1\\_D/SRTM/SRTMGL1.003/2000.02.11/](http://e4ftl01.cr.usgs.gov/MODV6_Da1_D/SRTM/SRTMGL1.003/2000.02.11/). We thank Fang zhao of the Wuhan University for his kind helps in revising our manuscript.

**Conflicts of Interest:** The authors declare no conflict of interest.

## References

1. Gao, L. Engineering Problems and Countermeasures of Land Reclamation in Tianjin Nangang Industrial Zone; Tianjin University: Tianjin, China, 2015.

2. Kooir, H. Land subsidence due to compaction in the coastal area of The Netherlands: the role of lateral fluid flow and constraints from well-log data. *Glob Planet Change*. **2000**, *27*, 207-222.
3. Jiang, L.; Lin, H. Integrated analysis of SAR interferometric and geological data for investigating long-term reclamation settlement of Chek Lap Kok Airport, Hong Kong. *Eng Geol*. **2010**, *110*(3-4), 77-92.
4. Liu, X.; Zhao, C.; Zhang, Q.; Yang, C.; Zhang, J. Characterizing and monitoring ground settlement of marine reclamation land of Xiamen New Airport, China with Sentinel-1 SAR datasets. *Remote Sens*. **2019**, *11*(5), 585.
5. Yu, Q.; Wang, Q.; Yan, X.; Yang, T.; Song, S.; Yao, M.; Zhou, K.; Huang, X. Ground deformation of the Chongming East Shoal Reclamation Area in Shanghai based on SBAS-InSAR and laboratory tests. *Remote Sens*. **2020**, *12*, 1016.
6. Yang, M.; Yang, T.; Zhang, L.; Lin, J.; Qin, X.; Liao, M. Spatio-temporal characterization of a reclamation settlement in the Shanghai coastal area with time series analyses of X-, C-, and L-band SAR datasets. *Remote Sens*. **2018**, *10*(2), 329.
7. Zhou, L.; Shi, X.; Ren, C.; Huang, Y.; Zhu, Z. Monitoring of Land Subsidence in Shenzhen Reclamation Area Based on Sentinel-1A Interferometric Synthetic Aperture Radar. *Science Technology and Engineering*. **2021**, *21*, 8765-8769.
8. Chen, G.; Zhang, Y.; Zeng, R.; Yang, Z.; Chen, X.; Zhao, F.; Meng, X. Detection of land subsidence associated with land creation and rapid urbanization in the Chinese Loess Plateau using time series InSAR: A case study of Lanzhou New District. *Remote Sens*. **2018**, *10*(2), 270.
9. Zhang, Y.; Liu, Y.; Jin, M.; Jing, Y.; Liu, Y.; Liu, Y.; Chen, Y. Monitoring land subsidence in Wuhan city (China) using the SBAS-InSAR method with radarsat-2 imagery data. *Remote Sens*. **2019**, *19*(3), 743.
10. Jiang, Y.; Liao, M.; Wang, H.; Zhang, L.; Balz, T. Monitoring land subsidence in Wuhan city (China) using the SBAS-InSAR method with radarsat-2 imagery data. *Sensors*. **2016**, *8*(12), 1021.
11. Cai, F.; Su, X.; Liu, J.; Li, B.; Lei, G. Coastal erosion in China under the condition of global climate change and measures for its prevention. *Prog. Nat. Sci*. **2009**, *19*(4), 415-426.
12. Ma, J.; Zhou, Z.; Guo, Q.; Zhu, S.; Dai, Y.; Shen, Q. Spatial characterization of seawater intrusion in a coastal Aquifer of Northeast Liaodong Bay, China. *Sustainability*. **2019**, *11*(24), 7013.
13. Dongmeia, H.; Currellc, M. Delineating multiple salinization processes in a coastal plain aquifer, northern China: Hydrochemical and isotopic evidence. *Hydrol Earth Syst Sci*. **2018**, *22*, 3473-3491.
14. Zhu, L.; Jiang, C.; Wang, Y.; Peng, Y.; Zhang, P. A risk assessment of water salinization during the initial impounding period of a proposed reservoir in Tianjin, China. *Sustainability*. **2013**, *15*(9), 1743-1751.
15. Bai, L.; Jiang, L.; Wang, H.; Sun, Q. Spatiotemporal Characterization of Land Subsidence and Uplift (2009-2010) over Wuhan in Central China Revealed by TerraSAR-X InSAR Analysis. *Remote Sens*. **2016**, *8*(4), 350.
16. Liu, P.; Li, Q.; Li, Z.; Hoey, T.; Liu, G.; Wang, C.; Hu, Z.; Zhou, Z.; Singleton, A. Anatomy of Subsidence in Tianjin from Time Series InSAR. *Remote Sens*. **2016**, *8*(3), 45-49.
17. Chen, Y. Study on a long sequence of groundwater level dynamic in Tianjin; China University of Geosciences (Beijing): Beijing, China, 2015.
18. Wang, K.; Wang, W.; Li, Q.; Yu, m.; Li, P. Characteristics of changes of groundwater buried depth and influencing factors in Tianjin plain area over past 21 years. *Water Resources Protection*. **2014**, *30*(3), 45-49.
19. Guo, L.; Gong, H.; Li, X.; Zhu, L.; Lv, W.; Lyu, M. Analysis of land subsidence changes on the Beijing Plain from 2004 to 2015. *Proceedings of the International Association of Hydrological Sciences*. **2020**, *382*, 291-296.
20. Ha, D.; Zheng, G.; Loaiciga, H.A.; Guo, W.; Zhou, H.; Chai, J. Long-term groundwater level changes and land subsidence in Tianjin, China. *Acta Geotech*. **2021**, *16*(4), 1303-1314.
21. Tang, W.; Zhan, W.; Jin, B.; Motagh, M.; Xu, Y. Spatial Variability of Relative Sea-Level Rise in Tianjin, China: Insight From InSAR, GPS, and Tide-Gauge Observations. *Remote Sens*. **2021**, *14*, 2621-2633.
22. Zhuo, G.; Dai, K.; Huang, H.; Li, S.; Shi, X.; Feng, Y.; Li, T.; Dong, X.; Deng, J. Evaluating Potential Ground Subsidence Geo-Hazard of Xiamen Xiang'an New Airport on Reclaimed Land by SAR Interferometry. *Sustainability*. **2020**, *12*(17), 6991.
23. Du, Q.; Li, G.; Chen, D.; Zhou, Y.; Qi, S.; Wu, G.; Chai, M.; Tang, L.; Jia, H.; Peng, W. SBAS-InSAR-Based Analysis of Surface Deformation in the Eastern Tianshan Mountains, China. *Front. Earth Sci*. **2021**, *9*, 729454.
24. Li, B.; Wang, Z.; An, J.; Zhou, C.; Ma, Y. STime-Series Analysis of Subsidence in Nanning, China, Based on Sentinel-1A Data by the SBAS InSAR Method. *PFG-J PHOTOGRAMM REM*. **2020**, *88*(3-4), 291-304.

25. Tao, Q.; Wang, F.; Guo, Z.; Hu, L.; Yang, C.; Liu, T. Accuracy verification and evaluation of small baseline subset (SBAS) interferometric synthetic aperture radar (InSAR) for monitoring mining subsidence. *INT J REMOTE SENS.* **2021**, *54*(1), 641–662.
26. Zhu, C.; Zhang, Y.; Zhang, J.; Zhang, L.; Long, S.; Wu, H. Recent subsidence in Tianjin, China: Observations from multi-looking TerraSAR-X InSAR from 2009 to 2013. *Int.J.Remote Sens.* **2019**, *36*(23), 5869–5886.
27. Liu, L.; Yuan, C. Analysis of ground subsidence in Tianjin Beijiang, Nanjiang and Dongjiang Port. *Journal of Waterway and Harbor.* **2019**, *40*(3), 338-343.
28. Hu, B.; Zhou, J.; Wang, J.; Chen, Z.; Wang, D.; Xu, S. Risk assessment of land subsidence at Tianjin coastal area in China. *Environ Earth Sci.* **2009**, *59*, 269–276.
29. Liu, S.P.; Shi, B.; Gu, K.; Zhang, C.C.; Yang, J.L.; Zhang, S.; Yang, P. Land subsidence monitoring in sinking coastal areas using distributed fiber optic sensing: A case study. *Natural Hazards.* **2020**, *103*, 3043-3061.
30. Yang, A.W.; Liu, Q.; Li, Z.L.; Experimental Study on the Effect of Inherent Anisotropy on Strength and Deformation of Soft Soil. *Journal of wuhan university of technology.* **2012**, *34*(08), 87-91.
31. Li, X.Y.; Cheng, L.; Sha, H.L. Remote sensing analysis of tidal flat utilization characteristic of Tianjin Binhai New Area. *MARINE SCIENCE BULLETIN.* **2021**, *40*(4), 379-386.
32. Zhu, G.; Xu, X. Annual Processes of Land Reclamation from the Sea Along the Northwest Coast of Bohai Bay During 1974 to 2010. *Scientia Geographica Sinica.* **2012**, *32*(8), 1006–1012.
33. Xu, B.; Feng, G.; Li, Z.; Wang, Q.; Wang, C.; Xie, R. Coastal subsidence monitoring associated with land reclamation using the point target based SBAS-InSAR method: A case study of Shenzhen, China. *Remote Sens.* **2016**, *8*(8), 1006–652.
34. Chen, Y.; Yu, S.; Tao, Q.; Liu, G.; Wang, L.; Wang, F. Accuracy verification and correction of D-InSAR and SBAS-InSAR in monitoring mining surface subsidenc. *Remote Sens.* **2021**, *13*(21), 4365.
35. Yao, J.; Yao, X.; Liu, X. Landslide detection and mapping based on SBAS-InSAR and PS-InSAR: A case study in Gongjue County, Tibet, China. *Remote Sens.* **2022**, *14*(19), 4728.
36. Chen, D.; Chen, H.; Zhang, W.; Cao, C.; Zhu, K.; Yuan, X.; Du, Y. Characteristics of the residual surface deformation of multiple abandoned mined-out areas based on a field investigation and SBAS-InSAR: A case study in Jilin, China. *Remote Sens.* **2020**, *12*(22), 3752.
37. Festa, D.; Bonano, M.; Casagli, N.; Confuorto, P.; De Luca, C.; Del Soldato, M.; Casu, F. Nation-wide mapping and classification of ground deformation phenomena through the spatial clustering of P-SBAS InSAR measurements: Italy case study. *ISPRS J. Photogramm. Remote Sens.* **2022**, *189*, 1-22.
38. Wu, Q.; Jia, C.; Chen, S.; Li, H. SBAS-InSAR based deformation detection of urban land, created from mega-scale mountain excavating and valley filling in the Loess Plateau: The case study of Yan'an City. *Remote Sens.* **2019**, *11*(14), 1673.
39. Zhu, D. A Dissertation Submitted in Partial Fulfillment of the Requirements for the Degree of Master of Science; Nanjing Normal University: Nanjing, China, 2016.
40. Zhang, Y.; Meng, X.; Jordan, C.; Novellino, A.; Dijkstra, T.; Chen, G. Investigating slow-moving landslides in the Zhouqu region of China using InSAR time series. *Remote Sens.* **2018**, *15*(7), 1299–1315.
41. Chen, F.; Lin, H.; Zhou, W.; Hong, T.; Wang, G. Investigating slow-moving landslides in the Zhouqu region of China using InSAR time series. *Remote Sens Environ.* **2013**, *138*, 10-18.
42. Zhao, X.; Wang, L.; Ma, Y.; Wang, J.; Yang, X.; Yang, X.; Xing, J.; Jin, B. Monitoring and analysis of surface deformation in land reclamation area based on SBAS-InSAR technology: Take Tianjin port for example. *Marine Science Bulletin.* **2022**, *02*, 17-30.

**Disclaimer/Publisher's Note:** The statements, opinions and data contained in all publications are solely those of the individual author(s) and contributor(s) and not of MDPI and/or the editor(s). MDPI and/or the editor(s) disclaim responsibility for any injury to people or property resulting from any ideas, methods, instructions or products referred to in the content.